Circulation: Cardiovascular Interventions

ORIGINAL ARTICLE

Morphological Changes of Anomalous Coronary Arteries From the Aorta During the Cardiac Cycle Assessed by IVUS in Resting Conditions

Giovanni Maria Formato, PhD; Mauro Luca Agnifili, MD; Luca Arzuffi, MD; Antonio Rosato, BEng; Valentina Ceserani, MEng; Karina Geraldina Zuniga Olaya, BSn; Francesco Secchi, MD, PhD; Miriam Deamici, BSc; Michele Conti, PhD; Ferdinando Auricchio, PhD; Francesco Bedogni, MD; Alessandro Frigiola, MD; Mauro Lo Rito, MD

BACKGROUND: Anomalous aortic origin of coronary artery (AAOCA) with intramural segment is associated with risk of sudden cardiac death, probably related to a compressive mechanism exerted by the aorta. However, the intramural compression occurrence and magnitude during the cardiac cycle remain unknown. We hypothesized that (1) in end diastole, the intramural segment is narrower, more elliptic, and has greater resistance than extramural segment; (2) the intramural segment experiences a further compression in systole; and (3) morphometry and its systolic changes vary within different lumen cross-sections of the intramural segment.

METHODS: Phasic changes of lumen cross-sectional coronary area, roundness (minimum/maximum lumen diameter), and hemodynamic resistance (Poiseuille law for noncircular sections) were derived from intravascular ultrasound pullbacks at rest for the ostial, distal intramural, and extramural segments. Data were obtained for 35 AAOCA (n=23 with intramural tract) after retrospective image-based gating and manual lumen segmentation. Differences between systolic and end-diastolic phases in each section, between sections of the same coronary, and between AAOCA with and without intramural tract were assessed by nonparametric statistical tests.

RESULTS: In end diastole, both the ostial and distal intramural sections were more elliptical ($P<0.001$) than the reference extramural section and the correspondent sections in AAOCA without intramural segment. In systole, AAOCA with intramural segment showed a flattening at the ostium (−6.76% [10.82%]; $P=0.024$) and a flattening (−5.36% [16.56%]; $P=0.011$), a narrowing (−4.62% [11.38%]; $P=0.020$), and a resistance increase (15.61% [30.07%]; $P=0.012$) at the distal intramural section. No-intramural sections did not show morphological changes during the entire cardiac cycle.

CONCLUSIONS: AAOCA with intramural segment has pathological segment-specific dynamic compression mainly in the systole under resting conditions. Studying AAOCA behavior with intravascular ultrasound during the cardiac cycle may help to evaluate and quantify the severity of the narrowing.

GRAPHIC ABSTRACT: A graphic abstract is available for this article.

Key Words: coronary vessel anomalies ■ diastole ■ heart ■ ischemia ■ sudden cardiac death ■ systole

There is a large body of evidence suggesting that the intramural segment is one of the most hemodynamics-threatening anatomic features of the anomalous aortic origin of the coronary arteries (AAOCA), posing patients at a higher risk of myocardial ischemia and sudden cardiac death (SCD) under physical effort.[1–6]

Correspondence to: Mauro Lo Rito, MD, Department of Congenital Cardiac Surgery, IRCCS Policlinico San Donato, Piazza Edmondo Malan 2, 20097, San Donato Milanese, Italy. Email mauro.lorito@gmail.com

Supplemental Material is available at https://www.ahajournals.org/doi/suppl/10.1161/CIRCINTERVENTIONS.122.012636.
For Sources of Funding and Disclosures, see page 424.

Circulation: Cardiovascular Interventions is available at www.ahajournals.org/journal/circinterventions

WHAT IS KNOWN

- Patients with anomalous aortic origin of the coronary artery are subjected to ischemia during effort due to the compression of anomalous segment such as the intramural.

WHAT THE STUDY ADDS

- Intravascular ultrasound imaging in anomalous aortic origin of the coronary artery allows systematic assessment of the dynamic component of compression during the cardiac cycle revealing which segment and in which cardiac phase is susceptible to narrowing.

Nonstandard Abbreviations and Acronyms

AAOCA	anomalous aortic origin of the coronary artery
IBG	image-based gating
IVUS	intravascular ultrasound
SCD	sudden cardiac death

Essentially, the intramural segment is affected by a fixed-anatomical and dynamic stenosis,[7,8] which means that the coronary lumen is generally narrower[9] and more elliptic[10] than the reference distal lumen and that such morphological characteristics can be further exacerbated during the cardiac cycle by a systolic lateral compression from the aorta.[11,12]

To fully elucidate the compression mechanism of the intramural segment, it is crucial to study the morphological changes and behavior of the anomalous coronary lumen during the whole cardiac cycle.

Coronary computed tomography imaging is adopted for diagnosis and anatomical risk profile definition of AAOCA[13]; however, its reliability to assess differences between cardiac cycle phases is controversial because the anomalous coronary lumen dimension, especially in the intramural segment, may reach the computed tomography spatial resolution.[12,14] Intracoronary imaging using optical coherence tomography or intravascular ultrasound (IVUS) empowers the interventionalist with high-resolution cross-sectional views of the coronary artery, although they are not widely adopted because it consists of an invasive procedure and may be technically challenging in AAOCA. On one hand, optical coherence tomography has a better axial resolution (10–20 µm) and a high pullback speed of 10 to 40 mm/s,[15] providing an instant picture of the entire coronary lumen. Applied to AAOCA, optical coherence tomography is not suitable for assessing differences among phases within the same cardiac cycle because it has an excessive pullback velocity. The IVUS, despite having a lower spatial resolution if compared with optical coherence tomography, allows studying coronary lumen morphological variations within the same cardiac cycle and has been suggested as the gold standard for the evaluation of the phasic morphological changes of AAOCA.[7,16,17]

We use IVUS imaging of subjects with AAOCA to assess the morphological changes of the anomalous coronary lumen and investigate whether there are differences between AAOCA with and without intramural segment to provide new insights in the pathogenic mechanism of compression. We hypothesize that (1) in the end diastole, the intramural segment is narrower, more elliptic, and has greater resistance than extramural segment; (2) the intramural segment experiences a compression during systole, which further reduces lumen area, increases the eccentricity, and increases the hemodynamic resistance; and (3) the morphometry and its systolic changes vary within different lumen cross-sections of the intramural segment.

METHODS

The data that support the findings of this study are available from the corresponding author upon reasonable request.

Study Population

This is an observational retrospective study conducted at IRCCS Policlinico San Donato (San Donato Milanese, Milan, Italy) including all patients with diagnosis of AAOCA who underwent coronary IVUS (n=39) between 2017 and 2022 according to institutional clinical guidelines. All IVUS procedures were performed with patients in resting conditions. The study was approved by the institutional review board (protocol number: 63/int/2019), and consent was obtained. For each candidate, an IVUS quality check was conducted to identify the segments adequate for the morphometric analysis using RadiAnt DICOM Viewer, version 2021.2.2 (Medixant). The IVUS was considered suitable for morphometric analysis only if it included the ostium, the intramural (if present), and the extramural tracts with the absence of evident vessel wall disease in the tract of interest. We excluded 4 patients because IVUS did not meet the selection criteria. The final cohort of the study included 35 subjects (Figure 1) in whom the IVUS was performed with commercially available 20-MHz solid-state transducer (Volcano Corporation, Philips Healthcare; n=24) or 40-MHz rotational transducer (Boston Scientific; n=11). Pullbacks were performed manually (n=24) or with a motorized system at a constant velocity of 1 mm/s (n=11). Images were acquired at 30 frames/s in digital format, saved according to DICOM standards, and stored into the picture archiving and communication system. Patients were divided according to the presence of the intramural segment into 2 groups: those with intramural tract (n=23, AAOCA-IM) and those without intramural tract (n=12, AAOCA-NO-IM). The intramural segment was first detected based on computed tomography. Transmural course,[18] that is, a short intramural segment, was considered intramural. The presence and the end of the intramural segment were also evaluated by visual analysis of IVUS images. The assessment was based essentially

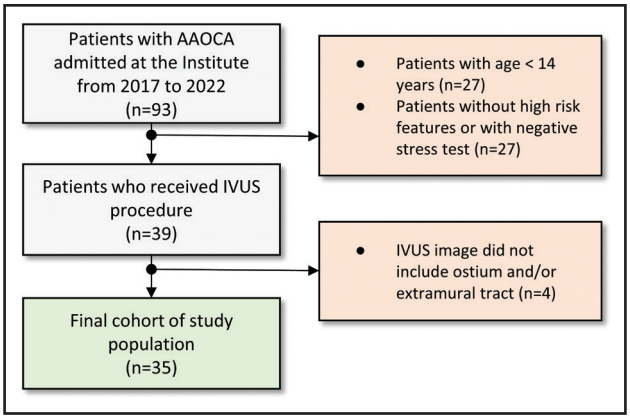

Figure 1. Flowchart of patient enrollment and final study population.
AAOCA indicates anomalous aortic origin of coronary artery; and IVUS, intravascular ultrasound.

on the following aspects: (1) the morphology of the lumen, in particular, the transition from elliptical to circular shape; (2) the absence/presence of the aortic lumen; (3) the absence/presence of side branches or vessel bifurcations. Table 1 summarizes the characteristics of the included subjects, as well as the types of the AAOCA for each group. We defined 3 coronary lumen cross-sections of interest for the morphometric analysis: (1) the coronary ostium (S_{OSTIAL}), (2) the distal end of the intramural segment (S_{MID}), and (3) the distal reference segment (S_{DISTAL}) before any major bifurcation. For the AAOCA-NO-IM, the S_{MID} was identified in the midportion in between the S_{OSTIAL} and S_{DISTAL} as a similar region of the S_{MID} for the AAOCA-IM.

IVUS Morphometric Analysis

The description of the coronary lumen morphometry in the whole cardiac cycle takes the following steps: (1) retrospective cardiac gating, (2) identification of the coronary segments of interest, (3) extraction of subsets of frames describing a full cardiac cycle, and (4) segmentation and morphometric analysis. All these IVUS imaging analyses were performed using specific scripts using MATLAB Image Processing Toolbox Release 2021b (MathWorks).

Because IVUS images are not ECG gated, the cardiac gating was performed along each IVUS pullback using a retrospective image-based gating (IBG) method previously validated and published.[19] Briefly, the method uses image characteristics, such as movement or pulsatility, to identify a stable phase that is likely to occur at the end of the diastole. The frames that are in correspondence of such phases are marked as end-diastolic frames; 2 consecutive end-diastolic frames define a subset of frames describing a full cardiac cycle (Figure 2A).

After retrospective IBG, each IVUS pullback was reviewed by 2 expert operators (G.M.F. and M.L.R.) in consensus, to identify 3 different subsets of frames, each enclosed between 2 consecutive end-diastolic frames, describing 3 full cardiac cycles recorded when the IVUS probe was pulled back in correspondence of the sections S_{DISTAL}, S_{MID}, and S_{OSTIAL} (Figure 2B).

We hypothesized that the length of the coronary tract spanned by the IVUS probe in one cardiac cycle (ie, between 2 end-diastolic frames) was sufficiently small to consider the tract as a single luminal cross-section. This hypothesis ensured that the observed luminal changes were uniquely due to aortic motion and pulsatile blood pressure and not to the axial movement of the IVUS transducer.[20]

All the frames of the sections S_{DISTAL}, S_{MID}, and S_{OSTIAL} were manually segmented by 1 expert operator (G.M.F.) by delineating the inner edge of the luminal-intimal interface. A subset of 887 of 2579 frames (34% of the total) from a sample of 12 of 35 patients (34% of the population) was also segmented by a blinded expert clinician (M.L.R.) to assess reproducibility and correctness of the measurements. Then, for each frame, we computed (1) the cross-sectional area (mm^2), (2) the minimum and maximum diameters (mm), (3) the roundness (minimum/maximum lumen diameter), and (4) the cross-sectional hemodynamic resistance from the law of Poiseuille for noncircular sections (mm^{-4})[8] (Figure 2C).

The measures in 1 cardiac cycle were fitted with a smoothing spline with a smoothing parameter of 0.7. We normalized the duration of each investigated cycle to 1 s (ie, a heart rate of 60 beats per minute) and defined an end-diastolic window from 0% to 2.5% and from 97.5% to 100% of the cardiac cycle and a systolic window going from 16% to 61% (amplitude, 45%) of the cardiac cycle based upon consideration of the normal PQ and QT durations.[19,21–24] Then, the lumen morphometry in the end-diastolic and systolic phases was characterized for each section by taking the mean of the measures over the corresponding windows, as well as percentage variations between systolic and end-diastolic phases (Figure 2D).

The details of the IBG method, coronary segment definition, and analysis are described in the Supplemental Material.

Table 1. Demographic Characteristics of the Study Population

	AAOCA-NO-IM (n=12)	AAOCA-IM (n=23)
Demographics		
Female sex, n (%)	4 (33%)	6 (26%)
Age, y	24 (24)	36 (28)
Anomaly, n (course)		
R-AAOCA	7	21
RCA from left sinus	6 (all interarterial)	20 (all interarterial)
RCA with high takeoff	1	1 (interarterial)
L-AAOCA	5	2
LCA from right sinus	2 (n=1 prepulmonic, n=1 subpulmonary)	2 (all interarterial)
LCA from noncoronary sinus	1 (retroaortic)	…
LCA from RCA	1 (subpulmonary)	…
CX from RCA	1 (retroaortic)	…

Age data are reported as median (interquartile range). Coronary anomaly is described in terms of anomalous coronary, origin, and course. AAOCA indicates anomalous aortic origin of coronary artery; CX, left circumflex coronary; IM, intramural; L, left; LCA, left coronary artery; R, right; and RCA, right coronary artery.

Statistical Analysis

Categorical data are reported as number and frequency. Considering the sample size and a non-normal distribution assessed by data visualization, continuous variables are summarized via median and interquartile range, and comparisons

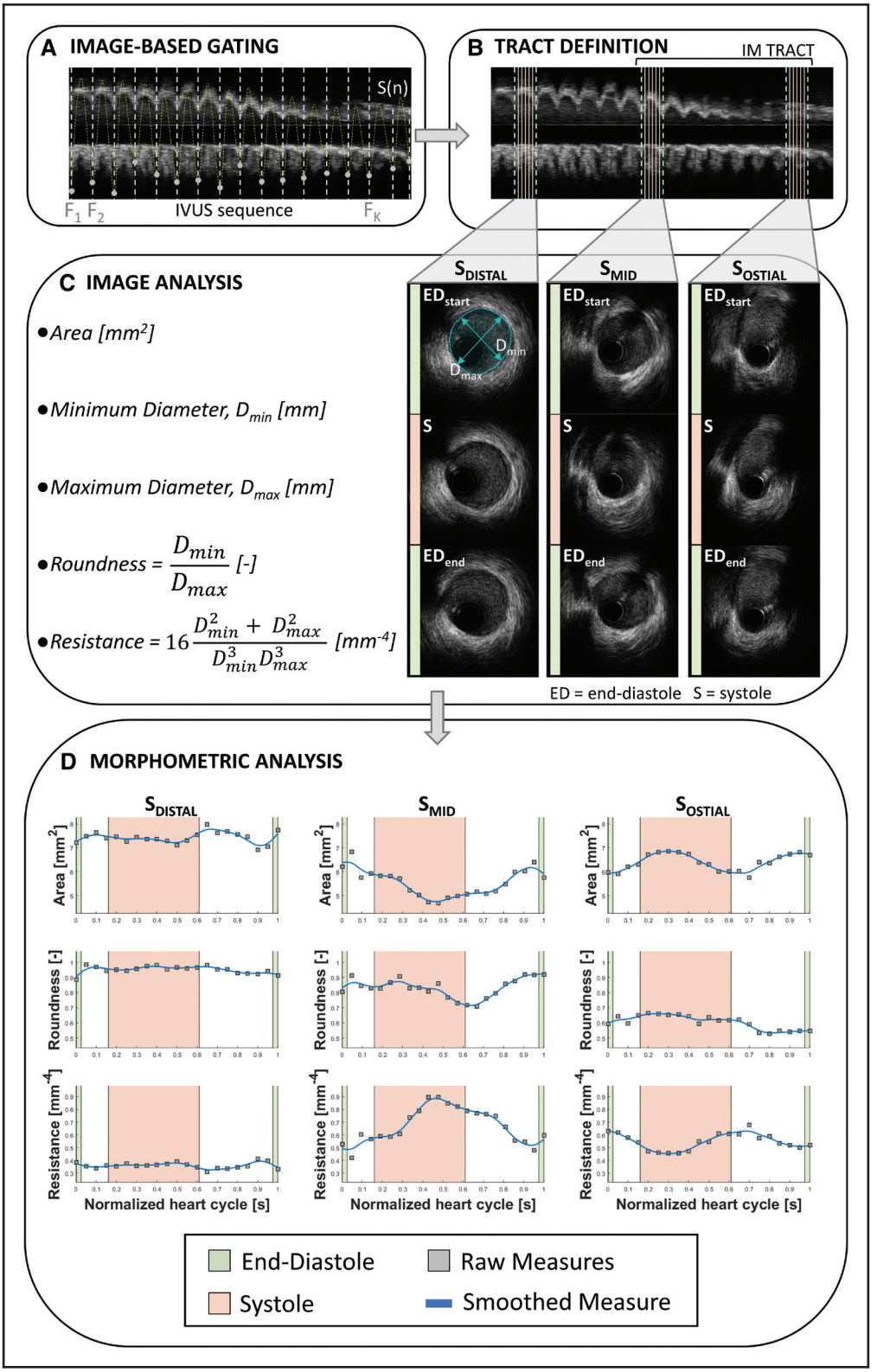

Figure 2. Methodological workflow to extract lumen morphometry in different phases of the cardiac cycle from ungated intravascular ultrasound (IVUS) pullbacks.

A, Image-based gating: for each IVUS sequence, a signal s(n) (idealized in yellow dashed line) was computed by combining image features, then the position of K local minima was manually identified to extrapolate a set of K end-diastolic (ED) frames F_K (vertical gray dashed lines) along the IVUS pullback. **B**, Tract definition: each IVUS pullback was reviewed by 2 expert operators to identify 3 different subsets of frames, each subset enclosed between 2 consecutive ED frames F_K and F_{K+1}. The retrieved subsets of frames describe full cardiac cycles of 3 small segments (also, sections) S_{DISTAL}, S_{MID}, and S_{OSTIAL} that are outside, distally inside, and at the ostium of the intramural (IM) tract of (*Continued*)

were performed using nonparametric statistical tests. Within each group, we did (1) comparisons between systolic and diastolic morphometry of each section to evaluate how each segment changed during the cardiac cycle and (2) comparisons between sections of the same coronary in both diastole and systole, to assess differences of the morphometry within each coronary. These comparisons were performed by Wilcoxon signed-rank tests. Then, using the Mann-Whitney *U* test, we compared homologous sections of AAOCA with and without intramural tract in both diastole and systole, to assess whether the observed morphometry and behavior were specific to the intramural segment.

Reproducibility and reliability of measures were assessed by interrater reproducibility tests between the primary rater (G.M.F.) and control rater (M.L.R.). Reproducibility of raw segmentations was assessed by the Jaccard index of similarity. Reproducibility of raw morphological measures was assessed by the intraclass correlation coefficient. Intraclass correlation coefficient estimates and their 95% CIs were calculated using a single rater, consistency, 2-way mixed-effects model.[25] *P* values were 2 sided; $P<0.05$ was considered statistically significant. Statistical tests were performed with the MATLAB Statistics and Machine Learning Toolbox (MathWorks), and intraclass correlation coefficient analysis was performed using the IBM SPSS statistical software, version 22 (IBM).

RESULTS

Study Population

From January 2017 to February 2022, we evaluated 93 patients with AAOCA at IRCCS Policlinico San Donato (Italy). We perform IVUS imaging in patients >14 years of age with high-risk anatomy or symptoms and provocative positive tests to elucidate anomalous coronary details. Therefore, among the 93 patients, we had 39 subjects who underwent IVUS evaluation (Figure 1). In 4 patients, the IVUS had an inadequate quality and was excluded. The final study cohort was formed by 35 patients with IVUS imaging that met the quality criteria and had all the segments of interest represented. The median age of the population was 32 (16) years, with predominantly right anomalous coronary artery (n=28), followed by left coronary artery (n=6) and anomalous circumflex artery (n=1). The anomalous coronary course and other details are resumed in Table 1. In the right AAOCA (n=28), we observed a right dominance in 23 (82%) patients and a left in 5 (18%). In the left AAOCA (n=7), the dominance was right in 6 (85.7%) and left in 1 patient. The posterior interventricular artery, which defined coronary dominance, originated from the anomalous coronary in 24 patients (68.5%) and the nonanomalous in 11 (31.5%). We divided the AAOCA population according to the presence of an intramural segment (n=23) or not intramural (n=12) for IVUS analysis. The first clinical manifestation that led to AAOCA diagnosis was cardiac related in 23 cases; meanwhile, it was an incidental finding in 12 asymptomatic subjects (Table S1).

For all 35 subjects with AAOCA, it was possible to proceed with IVUS image processing and segmentation with excellent results (104/105 [99%] cycles identified and 2511/2579 [97%] frames segmented) to obtain the variables of interest such as lumen area, diameters, roundness, and resistance in each of the 3 segments explored. The reproducibility analysis revealed a moderate-to-excellent agreement between raters based on intraclass correlation coefficient and Jaccard index. See the Supplemental Material for further details on the reproducibility analysis.

IBG revealed a mean heart frequency of 77±14 bpm across the data set. Overall, AAOCA showed a median lumen area of 8.8 (3.5) mm^2, a median lumen minimum diameter of 2.97 (0.98) mm, a median lumen maximum diameter of 3.91 (0.93) mm, a median roundness of 0.83 (0.26), and a median resistance of 0.29 (0.22) mm^{-4}. As further detailed in the following paragraphs, the morphometric analysis for each population group revealed that AAOCA-IM has a different behavior between segments and that these variations are significant compared with AAOCA-NO-IM. Results of the morphometric and statistical analysis are presented in Table 2, while boxplots of end-diastolic and systolic area, roundness, and resistance are depicted in Figures 3 through 5, respectively.

AAOCA With Intramural Segment

In end diastole, reference extramural section S_{DISTAL} had a median lumen area of 9.42 (3.73) mm^2, roundness of 0.91 (0.05), and resistance of 0.22 (0.20) mm^{-4}; mid intramural section S_{MID} had a median lumen area of 7.96 (2.92) mm^2, roundness of 0.77 (0.20), and resistance of 0.34 (0.19) mm^{-4}; ostial intramural section S_{OSTIAL} had a median lumen area of 7.87 (3.56) mm^2, roundness of 0.56 (0.25), and resistance of 0.37 (0.45) mm^{-4} (Table 2). S_{MID} had no significantly different area ($P=0.93$) and resistance ($P=0.96$) but was more elliptic ($P<0.001$) than S_{DISTAL}; in the same way, S_{OSTIAL} had no significantly different area ($P=0.30$) and resistance ($P=0.06$) than S_{DISTAL}

Figure 2 Continued. each AAOCA-IM, respectively. **C**, Image analysis: the coronary lumen was manually delineated in all frames of each section to extract the morphometric measures of area, minimum and maximum diameters, roundness, and resistance during the cardiac cycle. In the right side of the panel, 3 illustrative frames in the initial ED (ED_{start}), systole (S), and final ED (ED_{end}) of each cycle are depicted for each section. **D**, Morphometry extraction: raw measures (gray square dots) from each frame were then fitted by a smoothing spline (in blue). The obtained curve described the morphometric changes of the measure during the cardiac cycle. The curve was normalized to a duration of 1 s, systolic phase was estimated by considering a temporal window covering 45% of the cardiac cycle considering normal PQ and QT duration, ED phase was estimated considering the average of 2 windows covering 5% of the cardiac cycle at the start and end of the cycle. AAOCA indicates anomalous aortic origin of the coronary artery.

Table 2. End-Diastolic and Systolic Values of Area, Roundness, Minimum Diameter, Maximum Diameter, Resistance, and Their Percentage Systolic Variation, of AAOCA With and Without Intramural Segment

		AAOCA-NO-IM					AAOCA-IM					AAOCA-NO-IM vs AAOCA-IM		
		S_{DISTAL}	S_{MID}	S_{OSTIAL}	S_{MID} vs S_{DISTAL}	S_{OSTIAL} vs S_{DISTAL}	S_{DISTAL}	S_{MID}	S_{OSTIAL}	S_{MID} vs S_{DISTAL}	S_{OSTIAL} vs S_{DISTAL}	S_{DISTAL}	S_{MID}	S_{OSTIAL}
					P values*					*P* values*		*P* values		
Area, mm²	ED	9.65 (3.77)	9.90 (5.51)	9.96 (4.12)	1.00	1.00	9.42 (3.73)	7.96 (2.92)	7.87 (3.56)	0.93	0.30	0.77	0.29	0.058
	S	9.52 (3.47)	9.81 (4.03)	9.92 (4.77)	1.00	1.00	9.80 (3.63)	8.12 (2.44)	8.32 (3.45)	0.012	0.14	0.85	0.20	0.058
	V	−0.63 (8.19)	−4.11 (7.42)	−1.61 (10.91)	1.00	1.00	1.15 (6.16)	−4.62 (11.38)	−2.56 (7.07)	0.006	0.10	0.18	0.51	0.93
Roundness (–)	ED	0.94 (0.10)	0.88 (0.10)	0.84 (0.13)	0.54	0.08	0.91 (0.05)	0.77 (0.20)	0.56 (0.25)	<0.001	<0.001	0.43	0.003	<0.001
	S	0.92 (0.03)	0.89 (0.05)	0.87 (0.11)	0.81	0.33	0.90 (0.05)	0.72 (0.14)	0.50 (0.22)	<0.001	<0.001	0.24	<0.001	<0.001
	V	−1.32 (6.82)	0.05 (8.89)	2.64 (15.19)	1.00	0.90	−1.07 (5.00)	−5.36 (16.56)	−6.76 (10.82)	0.17	0.16	0.85	0.15	0.033
Resistance, mm⁻⁴	ED	0.22 (0.20)	0.20 (0.25)	0.21 (0.18)	1.00	1.00	0.22 (0.20)	0.34 (0.19)	0.37 (0.45)	0.96	0.06	0.79	0.16	0.023
	S	0.23 (0.20)	0.21 (0.22)	0.21 (0.24)	1.00	1.00	0.21 (0.19)	0.35 (0.19)	0.36 (0.51)	0.021	0.027	0.93	0.13	0.021
	V	1.36 (16.08)	8.86 (15.63)	5.93 (22.88)	0.45	1.00	−2.21 (9.89)	15.61 (39.07)	8.15 (22.19)	0.006	0.07	0.20	0.44	0.77
Minimum diameter, mm	ED	3.30 (0.82)	3.29 (0.98)	3.28 (0.75)	1.00	0.90	3.24 (0.57)	2.72 (0.56)	2.43 (1.07)	0.003	<0.001	0.66	0.018	0.005
	S	3.25 (0.74)	3.31 (0.81)	3.27 (0.96)	1.00	1.00	3.34 (0.55)	2.60 (0.62)	2.30 (0.87)	<0.001	<0.001	0.88	0.012	0.001
	V	0.43 (4.71)	−2.93 (7.77)	0.52 (5.26)	1.00	1.00	1.23 (5.27)	−8.34 (10.37)	−3.88 (8.02)	0.012	0.048	0.41	0.17	0.054
Maximum diameter, mm	ED	3.71 (0.61)	3.77 (0.91)	3.92 (0.69)	1.00	0.027	3.68 (0.71)	3.78 (1.01)	4.37 (0.83)	0.19	0.001	0.66	0.65	0.049
	S	3.63 (0.65)	3.81 (0.56)	4.00 (0.87)	0.54	0.08	3.68 (0.78)	3.92 (1.15)	4.53 (0.77)	0.08	<0.001	0.96	0.44	0.013
	V	1.00 (4.62)	−0.14 (5.26)	−4.10 (10.17)	1.00	1.00	1.57 (4.11)	−0.19 (10.74)	2.54 (6.44)	1.00	1.00	0.24	0.84	0.054

Comparisons between sections of the same coronary were done by Wilcoxon signed-rank tests. Comparisons between corresponding sections of AAOCA-IM and AAOCA-NO-IM were done by Mann-Whitney *U* tests. Values are presented as median (interquartile range). V presented in percentage. AAOCA indicates anomalous aortic origin of coronary artery; ED, end diastole; IM, intramural; S, systole; and V, systolic to end-diastolic variation.

*Bonferroni-corrected *P* values.[26]

but was more elliptic (*P*<0.001). In systole, S_{DISTAL} had median lumen area of 9.80 (3.63) mm², roundness of 0.90 (0.05), and resistance of 0.21 (0.19) mm⁻⁴; S_{MID} had a median lumen area of 8.12 (2.44) mm², roundness of 0.72 (0.14), and resistance of 0.35 (0.19) mm⁻⁴; ostial intramural section S_{OSTIAL} had median lumen area of 8.32 (3.45) mm², roundness of 0.50 (0.22), and resistance of 0.36 (0.51) mm⁻⁴. S_{MID} was narrower (*P*=0.012), more elliptic (*P*<0.001), and had a higher resistance (*P*=0.021) than S_{DISTAL}; S_{OSTIAL} was not narrower (*P*=0.14) but more elliptic (*P*<0.001) and with a higher resistance (*P*=0.027) than S_{DISTAL} (Table 2).

Sections inside the intramural segment showed changes of morphometry and hemodynamic resistance between systolic and end-diastolic phases (Figures 3 through 5). In particular, S_{MID} had a systolic narrowing of −4.62% (*P*=0.020), a systolic flattening of −5.36% (*P*=0.011), and a systolic increase of resistance of +15.61% (*P*=0.012); S_{OSTIAL} showed only a systolic flattening of −6.76% (*P*=0.024) but no significant changes of cross-sectional area (*P*=0.18) and resistance (*P*=0.15). Furthermore, the reference extramural section S_{DISTAL} did not show significant changes of morphometry and resistance between systolic and end-diastolic phases.

AAOCA Without Intramural Segment

In end diastole, reference section S_{DISTAL} had a median lumen area of 9.65 (3.77) mm², roundness of 0.94 (0.10), resistance of 0.22 (0.20) mm⁻⁴; mid section S_{MID} had median lumen area of 9.90 (5.51) mm², roundness of 0.88 (0.10), and resistance of 0.20 (0.25) mm⁻⁴; ostial section S_{OSTIAL} had median lumen area of 9.96 (4.12)

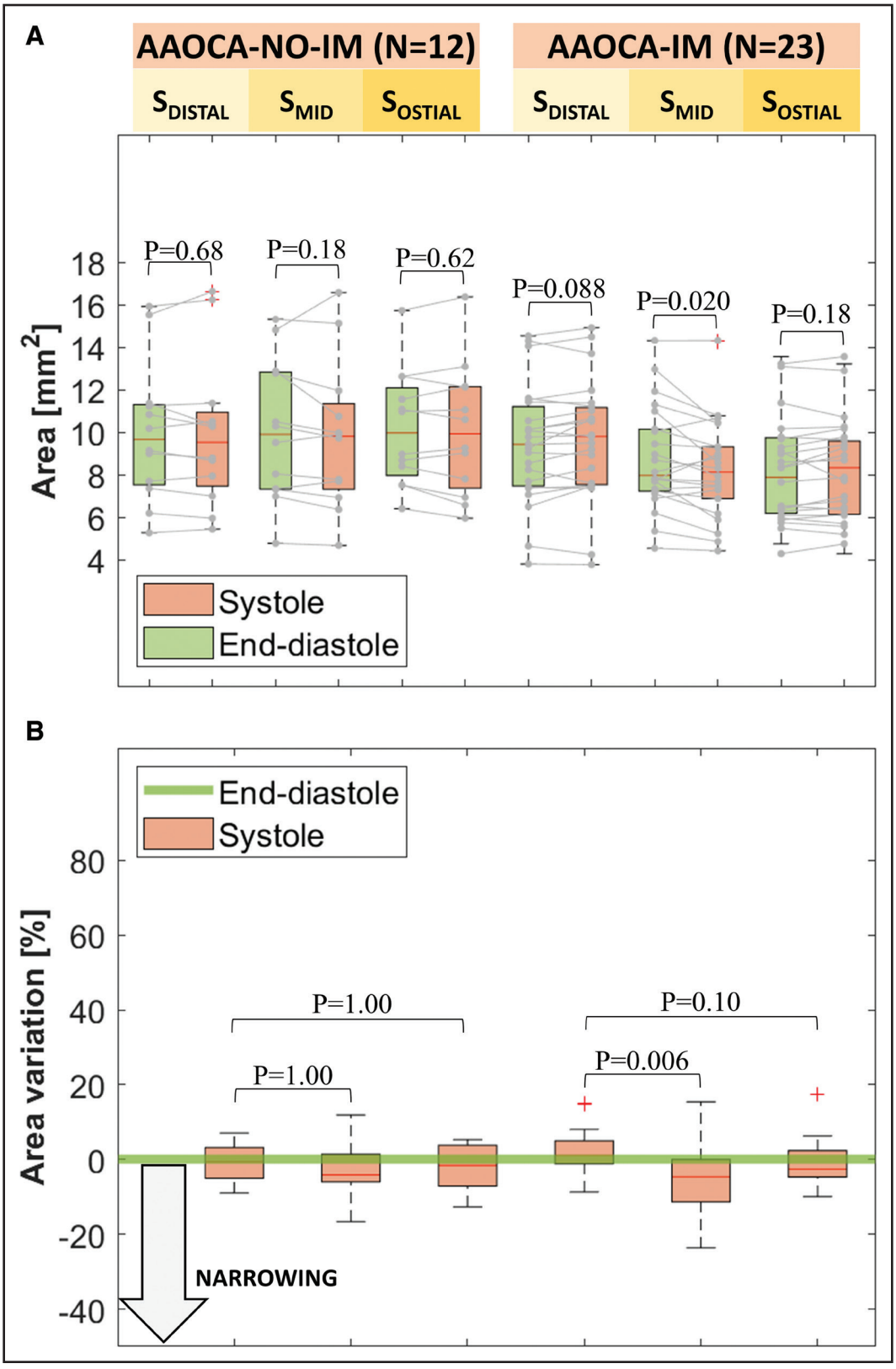

Figure 3. End-diastolic area, systolic area, and percentage systolic area variation in anomalous aortic origin of coronary arteries (AAOCA) with and without intramural (IM) segment.

A, Box plots (median, 25th and 75th percentiles, minimum and maximum values) of end-diastolic and systolic area of sections S_{DISTAL}, S_{MID}, and S_{OSTIAL}. Comparisons between phases are made by 2-sided Wilcoxon signed-rank tests. **B**, Box plots of percentage systolic area variation of sections S_{DISTAL}, S_{MID}, and S_{OSTIAL}. Comparisons between sections of the same coronary are made by 2-sided Wilcoxon signed-rank tests (Bonferroni-corrected *P* values).

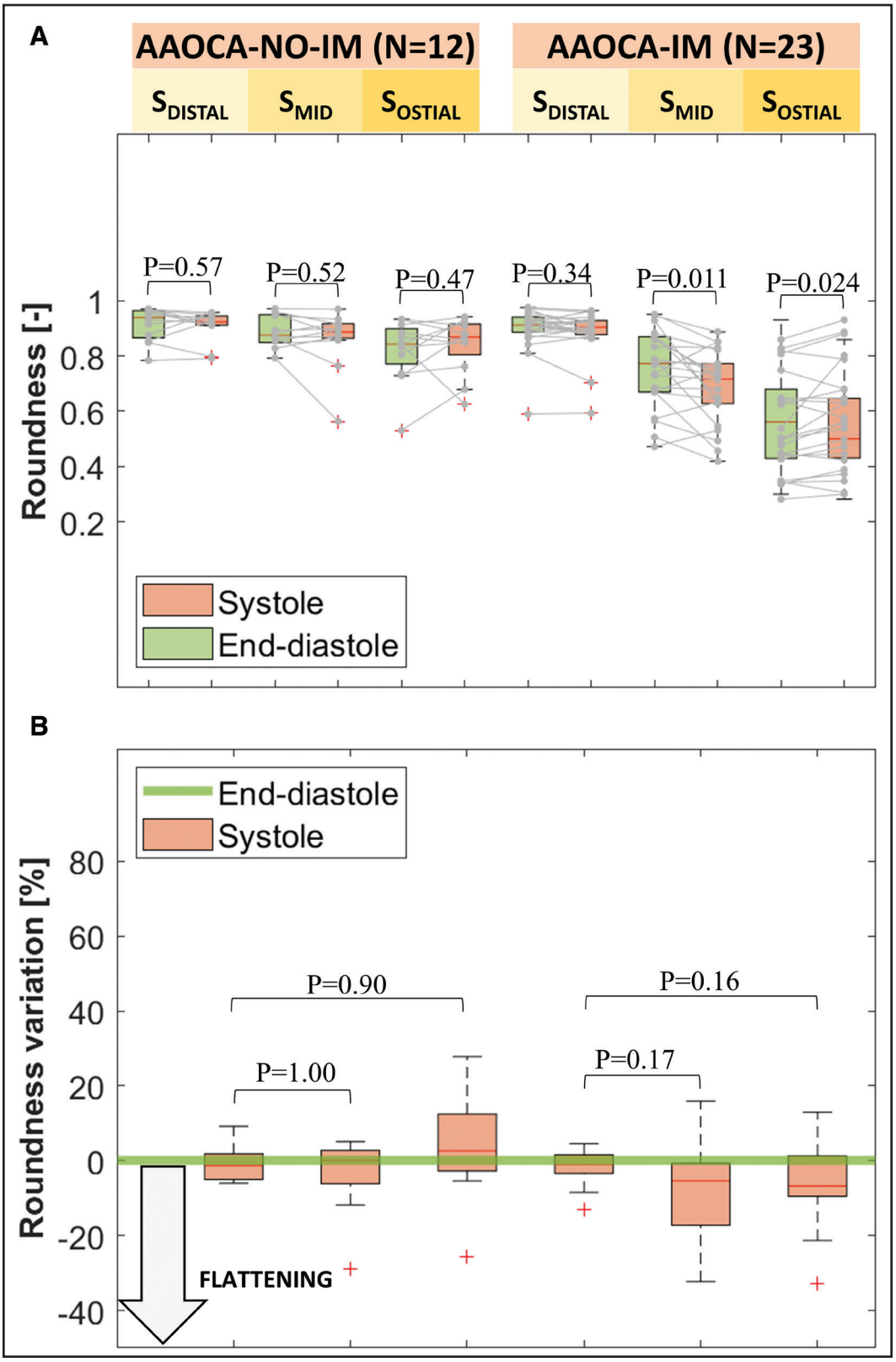

Figure 4. End-diastolic roundness, systolic roundness, and percentage systolic roundness variation in anomalous aortic origin of coronary arteries (AAOCA) with and without intramural (IM) segment.
A, Box plots (median, 25th and 75th percentiles, minimum and maximum values) of end-diastolic and systolic roundness of sections S_{DISTAL}, S_{MID}, and S_{OSTIAL}. Comparisons between phases are made by 2-sided Wilcoxon signed-rank tests. **B**, Box plots of percentage systolic roundness variation of sections S_{DISTAL}, S_{MID}, and S_{OSTIAL}. Comparisons between sections of the same coronary are made by 2-sided Wilcoxon signed-rank tests (Bonferroni-corrected *P* values).

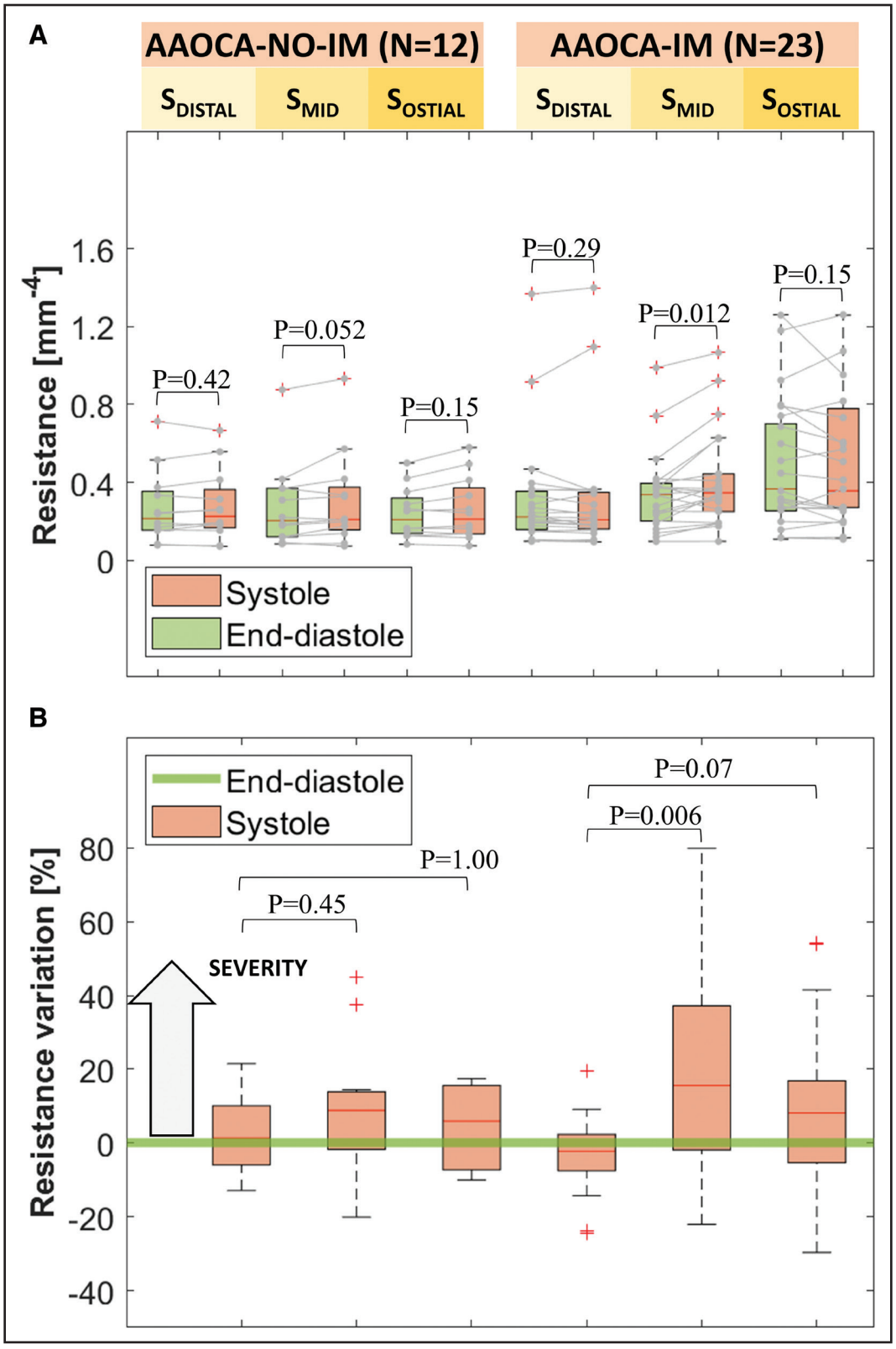

Figure 5. End-diastolic resistance, systolic resistance, and percentage systolic resistance variation in anomalous aortic origin of coronary arteries (AAOCA) with and without intramural (IM) segment.
A, Box plots (median, 25th and 75th percentile, minimum and maximum values) of end-diastolic and systolic resistance of sections S_{DISTAL}, S_{MID}, and S_{OSTIAL}. Comparisons between phases are made by 2-sided Wilcoxon signed-rank tests. **B**, Box plots of percentage systolic resistance variation of sections S_{DISTAL}, S_{MID}, and S_{OSTIAL}. Comparisons between sections of the same coronary are made by 2-sided Wilcoxon signed-rank tests (Bonferroni-corrected *P* values).

mm^2, roundness of 0.84 (0.13), and resistance of 0.21 (0.18) mm^{-4} (Table 2). S_{MID} had no significantly different area (P=1.00), roundness (P=0.54), and resistance (P=1.00) than S_{DISTAL}; similarly, S_{OSTIAL} had no significantly different area (P=1.00), roundness (P=0.08), and resistance (P=1.00) than S_{DISTAL}. In systole, S_{DISTAL} had a median lumen area of 9.52 (3.47) mm^2, roundness of 0.92 (0.03), and resistance of 0.23 (0.20) mm^{-4}; S_{MID} had a median lumen area of 9.81 (4.03) mm^2, roundness of 0.89 (0.05), and resistance of 0.21 (0.22) mm^{-4}; S_{OSTIAL} had a median lumen area of 9.92 (4.77) mm^2, roundness of 0.87 (0.11), and resistance of 0.21 (0.24) mm^{-4}. S_{MID} had no significantly different area (P=1.00), roundness (P=0.81), and resistance (P=1.00) than S_{DISTAL}; S_{OSTIAL} had no significantly different area (P=1.00), roundness (P=0.33), and resistance (P=1.00) than S_{DISTAL}.

Furthermore, neither S_{DISTAL}, nor S_{MID}, nor S_{OSTIAL} of AAOCA-NO-IM showed significant changes of morphometry and resistance between systolic and end-diastolic phases (Figures 3 through 5).

Comparisons Between AAOCA-IM and AAOCA-NO-IM

Finally, comparisons between AAOCA-IM and AAOCA-NO-IM showed peculiar morphometric characteristics and behavior specific of the intramural segment.

In end diastole, S_{DISTAL} of AAOCA-IM had no significantly different area (P=0.77), roundness (P=0.43), and resistance (P=0.79) than AAOCA-NO-IM; S_{MID} of AAOCA-IM had no significantly different area (P=0.29) and resistance (P=0.16) than AAOCA-NO-IM but was more eccentric (P=0.003); S_{OSTIAL} of AAOCA-IM had no significantly different area (P=0.058) than AAOCA-NO-IM but was more eccentric (P<0.001) and had higher resistance (P=0.023). In systole, S_{DISTAL} of AAOCA-IM had no significantly different area (P=0.85), roundness (P=0.24), and resistance (P=0.93) than AAOCA-NO-IM; S_{MID} of AAOCA-IM had no significantly different area (P=0.20) and resistance (P=0.13) than AAOCA-NO-IM but was more eccentric (P<0.001); S_{OSTIAL} of AAOCA-IM had no significantly different area (P=0.058) than AAOCA-NO-IM but was more eccentric (P<0.001) and had higher resistance (P=0.021).

DISCUSSION

AAOCA is a group of congenital heart diseases associated with SCD during physical activity. The pathogenetic mechanism is only partially elucidated; however, it is known that the presence of the intramural segment (ie, when the anomalous coronary runs proximally inside the aortic wall) poses patients at a higher risk because the intramural segment is generally hypoplastic, eccentric, and is further compressed during the systolic expansion of the aorta. The ostium is considered the section of maximum stenosis, but another possible area of narrowing proposed is the segment in the passage between the intramural and extramural parts.[7] These findings, together with the fact that the length of the intramural segment is considered one of the major risk factors of SCD, suggest that the whole intramural tract should be studied along the cardiac cycle. During cardiac cycle, aortic pressure variation between systole and diastole leads to phasic compression of the coronary; although to demonstrate, this mechanism, herein described at rest, may be considered as a small-scale version of the mechanism observed under effort, when aortic pressure increases and AAOCA lumen narrowing may lead to SCD. Studying lumen changes of AAOCA at different coronary segments and aortic pressures is, therefore, fundamental to elucidate which might be the mechanism of lumen narrowing in AAOCA.[27] IVUS is considered the gold standard imaging because it provides high spatial and temporal definition and allows assessment of the phasic morphological changes of AAOCA in the cardiac cycle.[7,16,17]

With the present investigation, we analyzed 3 different lumen cross-sections of the anomalous coronary artery: the ostium, the distal part of the intramural tract, and the round reference extramural section. We investigated the different behaviors of the 3 sections during diastole and systole in AAOCA with and without intramural tract. The analysis focused on the morphometric characteristics but also evaluated a surrogate of the hemodynamic resistance in order to infer how the geometrical changes may functionally impact the hemodynamics of AAOCA.[8]

The major finding of the present study is that AAOCA with intramural tract has a dynamic stenosis given by a compression of the intramural segment due to aorta expansion in systole, which increases the severity of the stenosis along the whole intramural length, even under resting conditions. These findings, for the first time, quantify objectively the geometric variation of coronary lumen during a cardiac cycle at rest and identify the different culprit areas where, and when, the dynamic compression is likely to occur.

More specifically, we observed that in end diastole, the intramural segment was more elliptical but had a comparable caliber and resistance than the reference extramural tract. During the cardiac cycle, while the ostium experienced only a systolic flattening (−6.76%), the distal intramural segment showed greater geometrical variations in terms of systolic flattening (−5.36%) and narrowing (−4.62%). These systolic changes added to the end-diastolic configuration, producing an intramural segment that was more elliptical along its whole length and narrower at the distal intramural segment. From a functional viewpoint, in systole, the distal intramural section resistance incremented by 15.61%, such that in this phase both the distal intramural section and the ostium had higher resistance than reference extramural section. Interestingly, the observed changes were specific to the

intramural segment, as no compression, flattening, or increase in resistance was observed either in the distal reference extramural section of AAOCA-IM or in any section of AAOCA-NO-IM.

Our results shed new light on the possible pathogenic mechanism of AAOCA with the intramural tract. The ostium is more elliptic and has little variation in terms of cross-sectional luminal area during the whole cardiac cycle, confirming previous studies that suggest the ostium as site of greater narrowing.[7] The elliptical shape and reduced variation support the correlation between ostial anatomical features (eg, slit-like ostial ridge) and ischemia or SCD.[6,10,28] Since the severity of a stenosis depends on the lumen caliber and length, these findings demonstrate that the intramural segment may have an adverse hemodynamic effect predominantly in systole due to the combined effect of the ostium and the intramural tract, supplementing the accepted theory that only intramural length is associated with ischemic risk in AAOCA[6,9] and that worst clinical outcomes occur at effort when diastolic phase shortens and systolic phase becomes important for myocardial perfusion.[29] Indeed, the mechanisms herein elucidated describe AAOCA at rest; however, we can hypothesize that such mechanisms would be magnified at effort as systolic compression increases due to higher aortic pressure. While the observed systolic morphometric changes of the intramural segment are potentially hemodynamics-threatening, we did not observe any opposite, that is, hemodynamics-favorable, behavior in AAOCA without intramural segment, although lumen expansion has been measured in normal epicardial coronary arteries.[30]

Study Limitations

This was a retrospective, observational, single-center, nonrandomized study conducted on a relatively small population (n=35). All subjects had AAOCA, group stratification was based only on the presence of the intramural segment, and there was not a control group of healthy subjects. Furthermore, population group size was not balanced (the AAOCA-IM group consisted of n=23 subjects). IVUS images were acquired with both manual and motorized pullbacks, potentially affecting the hypotheses that the coronary tract in the cardiac cycle is small enough to neglect any axial morphometric changes; this aspect could be controlled by keeping the transducer steady at the segment of interest, and further applying retrospective registration methods to compensate for the axial movement of the catheter.[31] Another limitation concerns the method used to extrapolate cardiac cycles along the IVUS pullbacks. The performance of the IBG is affected by image quality and parameter settings,[19] potentially hindering the reliability of the phase estimation. We, therefore, selected only IVUS images with good quality and considered only the images where the IBG signal peaks were easily identifiable. Finally, we described the behavior of the intramural segment only at rest, but worst systolic compression and SCD is related to effort. Consequently, the measured coronary morphometry and systolic changes might be smaller than that observed during the pathogenesis of AAOCA. A further step will be to assess morphometric changes of the intramural segment under effort using dobutamine infusion[16] or by means of computational simulations.[32–35]

Conclusions

AAOCA with proximal intramural tract has pathological fixed stenosis at the ostium and dynamic compression of the intramural segment mainly in systole. This finding, although measured in resting conditions, stresses the importance of the intramural evaluation through IVUS imaging during the cardiac cycle focused on morphological assessment of the ostium and of the intramural segment. Further investigations should be conducted to explore the potential correlation between morphological changes during the cardiac cycle at rest and under effort conditions and, if possible, correlate them with clinical manifestation and outcome.

ARTICLE INFORMATION

Received October 7, 2022; accepted June 6, 2023.

Affiliations

3D and Computer Simulation Laboratory (G.M.F., A.R.), Department of Clinical and Interventional Cardiology (M.L.A., L.A., M.D., F.B.), Department of Congenital Cardiac Surgery (K.G.Z.O., A.F., M.L.R.), and Department of Radiology (F.S.), IRCCS Policlinico San Donato, Milan, Italy. Department of Civil Engineering and Architecture, University of Pavia, Italy (V.C., M.C., F.A.). Department of Biomedical Sciences for Health, Università degli Studi di Milano, Milan, Italy (F.S.).

Sources of Funding

This work was supported by IRCCS Policlinico San Donato, a Clinical Research Hospital partially funded by the Italian Ministry of Health.

Disclosures

Dr Bedogni is a speaker/on the Speaker's Bureau (modest) for Medtronic, Boston Scientific, Abbott, and Terumo. The other authors report no conflicts.

Supplemental Material

Supplemental Methods
Supplemental Results
Tables S1–S3

REFERENCES

1. Taylor AJ, Rogan KM, Virmani R. Sudden cardiac death associated with isolated congenital coronary artery anomalies. *J Am Coll Cardiol*. 1992;20:640–647. doi: 10.1016/0735-1097(92)90019-j
2. Maron BJ, Shirani J, Poliac LC, Mathenge R, Roberts WC, Mueller FO. Sudden death in young competitive athletes: clinical, demographic, and pathological profiles. *JAMA*. 1996;276:199–204.
3. Taylor AJ, Byers JP, Cheitlin MD, Virmani R. Anomalous right or left coronary artery from the contralateral coronary sinus: "high-risk" abnormalities in the initial coronary artery course and heterogeneous clinical outcomes. *Am Heart J*. 1997;133:428–435. doi: 10.1016/s0002-8703(97)70184-4
4. Basso C, Maron BJ, Corrado D, Thiene G. Clinical profile of congenital coronary artery anomalies with origin from the wrong aortic sinus

leading to sudden death in young competitive athletes. *J Am Coll Cardiol*. 2000;35:1493–1501. doi: 10.1016/s0735-1097(00)00566-0
5. Eckart RE, Scoville SL, Campbell CL, Shry EA, Stajduhar KC, Potter RN, Pearse LA, Virmani R. Sudden death in young adults: a 25-year review of autopsies in military recruits. *Ann Intern Med*. 2004;141:829–834. doi: 10.7326/0003-4819-141-11-200412070-00005
6. Jegatheeswaran A, Devlin PJ, McCrindle BW, Williams WG, Jacobs ML, Blackstone EH, DeCampli WM, Caldarone CA, Gaynor JW, Kirklin JK, et al. Features associated with myocardial ischemia in anomalous aortic origin of a coronary artery: a Congenital Heart Surgeons' Society study. *J Thorac Cardiovasc Surg*. 2019;158:822–834.e3. doi: 10.1016/j.jtcvs.2019.02.122
7. Angelini P, Uribe C. Critical update and discussion of the prevalence, nature, mechanisms of action, and treatment options in potentially serious coronary anomalies. *Trends Cardiovasc Med*. 2022;S1050-1738(22)00074-3. doi:10.1016/j.tcm.2022.05.007
8. Bigler MR, Ashraf A, Seiler C, Praz F, Ueki Y, Windecker S, Kadner A, Räber L, Gräni C. Hemodynamic relevance of anomalous coronary arteries originating from the opposite sinus of valsalva-in search of the evidence. *Front Cardiovasc Med*. 2021;7:591326.
9. Kaushal S, Backer CL, Popescu AR, Walker BL, Russell HM, Koenig PR, Rigsby CK, Mavroudis C. Intramural coronary length correlates with symptoms in patients with anomalous aortic origin of the coronary artery. *Ann Thorac Surg*. 2011;92:986–91; discussion 991. doi: 10.1016/j.athoracsur.2011.04.112
10. Harris MA, Whitehead KK, Shin DC, Keller MS, Weinberg PM, Fogel MA. Identifying abnormal ostial morphology in anomalous aortic origin of a coronary artery. *Ann Thorac Surg*. 2015;100:174–179. doi: 10.1016/j.athoracsur.2015.02.031
11. Angelini P, Flamm SD. Newer concepts for imaging anomalous aortic origin of the coronary arteries in adults. *Catheter Cardiovasc Interv*. 2007;69:942–954. doi: 10.1002/ccd.21140
12. Zhang LJ, Wu SY, Huang W, Zhou CS, Lu GM. Anomalous origin of the right coronary artery originating from the left coronary sinus of valsalva with an interarterial course: diagnosis and dynamic evaluation using dual-source computed tomography. *J Comput Assist Tomogr*. 2009;33:348–353. doi: 10.1097/rct.0b013e318184cdb0
13. Cheezum MK, Ghoshhajra B, Bittencourt MS, Hulten EA, Bhatt A, Mousavi N, Shah NR, Valente AM, Rybicki FJ, Steigner M, et al. Anomalous origin of the coronary artery arising from the opposite sinus: prevalence and outcomes in patients undergoing coronary CTA. *Eur Heart J Cardiovasc Imaging*. 2017;18:224–235. doi: 10.1093/ehjci/jev323
14. Linsen PVM, Kofflard MJM, Lam SW, Kock MCJM. First in humans: dobutamine stress cardiac computed tomography to evaluate dynamic compression of an anomalous left coronary artery. *Coron Artery Dis*. 2018;29:607–608. doi: 10.1097/MCA.0000000000000641
15. Araki M, Park SJ, Dauerman HL, Uemura S, Kim JS, Di Mario C, Johnson TW, Guagliumi G, Kastrati A, Joner M, et al. Optical coherence tomography in coronary atherosclerosis assessment and intervention. *Nat Rev Cardiol*. 2022;19:684–703. doi: 10.1038/s41569-022-00687-9
16. Angelini P, Uribe C, Monge J, Tobis JM, Elayda MA, Willerson JT. Origin of the right coronary artery from the opposite sinus of Valsalva in adults: characterization by intravascular ultrasonography at baseline and after stent angioplasty: characterization of ACAOS by IVUS. *Catheter Cardiovasc Interv*. 2015;86:199–208. doi: 10.1002/ccd.26069
17. Angelini P, Uribe C. Anatomic spectrum of left coronary artery anomalies and associated mechanisms of coronary insufficiency. *Catheter Cardiovasc Interv*. 2018;92:313–321. doi: 10.1002/ccd.27656
18. Bigler MR, Kadner A, Räber L, Ashraf A, Windecker S, Siepe M, Padalino MA, Gräni C. Therapeutic management of anomalous coronary arteries originating from the opposite sinus of valsalva: current evidence, proposed approach, and the unknowing. *J Am Heart Assoc*. 2022;11:e027098. doi: 10.1161/JAHA.122.027098
19. Maso Talou GD, Larrabide I, Blanco PJ, Bezerra CG, Lemos PA, Feijoo RA. Improving cardiac phase extraction in IVUS studies by integration of gating methods. *IEEE Trans Biomed Eng*. 2015;62:2867–2877. doi: 10.1109/TBME.2015.2449232
20. Arbab-Zadeh A, DeMaria AN, Penny WF, Russo RJ, Kimura BJ, Bhargava V. Axial movement of the intravascular ultrasound probe during the cardiac cycle: implications for three-dimensional reconstruction and measurements of coronary dimensions. *Am Heart J*. 1999;138:865–872. doi: 10.1016/s0002-8703(99)70011-6
21. Malik M, Färbom P, Batchvarov V, Hnatkova K, Camm AJ. Relation between QT and RR intervals is highly individual among healthy subjects: implications for heart rate correction of the QT interval. *Heart*. 2002;87:220–228. doi: 10.1136/heart.87.3.220
22. Malik M, Hnatkova K, Sisakova M, Schmidt G. Subject-specific heart rate dependency of electrocardiographic QT, PQ, and QRS intervals. *J Electrocardiol*. 2008;41:491–497. doi: 10.1016/j.jelectrocard.2008.06.022
23. Surawicz B, Knilans TK, Chou TC. *Chou's Electrocardiography in Clinical Practice: Adult and Pediatric*. 6th ed. Saunders/Elsevier; 2008.
24. Toman O, Hnatkova K, Smetana P, Huster KM, Šišáková M, Barthel P, Novotný T, Schmidt G, Malik M. Physiologic heart rate dependency of the PQ interval and its sex differences. *Sci Rep*. 2020;10:2551. doi: 10.1038/s41598-020-59480-8
25. Koo TK, Li MY. A guideline of selecting and reporting intraclass correlation coefficients for reliability research. *J Chiropr Med*. 2016;15:155–163. doi: 10.1016/j.jcm.2016.02.012
26. Li G, Taljaard M, Van den Heuvel ER, Levine MAH, Cook DJ, Wells GA, Devereaux PJ, Thabane L. An introduction to multiplicity issues in clinical trials: the what, why, when and how. *Int J Epidemiol*. 2017;46:746–755. doi:10.1093/ije/dyw320
27. Formato GM, Lo Rito M, Auricchio F, Frigiola A, Conti M. Aortic expansion induces lumen narrowing in anomalous coronary arteries: a parametric structural finite element analysis. *J Biomech Eng*. 2018;140:111008. doi: 10.1115/1.4040941
28. Virmani R, Chun PKC, Goldstein RE, Robinowitz M, Mcallister HA. Acute takeoffs of the coronary arteries along the aortic wall and congenital coronary ostial valve-like ridges: association with sudden death. *J Am Coll Cardiol*. 1984;3:766–771. doi: 10.1016/s0735-1097(84)80253-3
29. Klabunde RE. *Cardiovascular Physiology Concepts*. 2nd ed. Lippincott Williams & Wilkins/Wolters Kluwer; 2012.
30. Weissman NJ, Palacios IF, Weyman AE. Dynamic expansion of the coronary arteries: implications for intravascular ultrasound measurements. *Am Heart J*. 1995;130:46–51. doi: 10.1016/0002-8703(95)90234-1
31. Talou GDM, Blanco PJ, Larrabide I, Bezerra CG, Lemos PA, Feijoo RA. Registration methods for IVUS: transversal and longitudinal transducer motion compensation. *IEEE Trans Biomed Eng*. 2017;64:890–903. doi: 10.1109/TBME.2016.2581583
32. Razavi A, Sachdeva S, Frommelt PC, LaDisa JF. Patient-specific numerical analysis of coronary flow in children with intramural anomalous aortic origin of coronary arteries. *Semin Thorac Cardiovasc Surg*. 2021;33:155–167. doi: 10.1053/j.semtcvs.2020.08.016
33. Cong M, Zhao H, Dai S, Chen C, Xu X, Qiu J, Qin S. Transient numerical simulation of the right coronary artery originating from the left sinus and the effect of its acute take-off angle on hemodynamics. *Quant Imaging Med Surg*. 2021;11:2062–2075. doi: 10.21037/qims-20-125
34. Lo Rito M, Romarowski RM, Rosato A, Pica S, Secchi F, Giamberti A, Auricchio F, Frigiola A, Conti M. Anomalous aortic origin of coronary artery biomechanical modeling: toward clinical application. *J Thorac Cardiovasc Surg*. 2021;161:191–201.e1. doi: 10.1016/j.jtcvs.2020.06.150
35. Rigatelli G, Zuin M. Computed tomography-based patient-specific biomechanical and fluid dynamic study of anomalous coronary arteries with origin from the opposite sinus and intramural course. *Heart Int*. 2020;14:105–111. doi: 10.17925/HI.2020.14.2.105